

Design and Implementation of 76W Forward Converter with Dual output to power Up digit unit for space application

Poornima Mernal ^a, Umavathi.M ^b, Santhosh B L ^c, Prakash G ^d, B K Singh^{e,*}

^a M.Tech PE, Dept of EEE,BMSCE Bengaluru, India

^b Assistant Professor,Dept of EEE,BMSCE Bengaluru, India

^c Assistant Manager,Centum Electronics Ltd.

^d Engineer,Centum Electronics Ltd.

^e Director, Centum Electronics Ltd.

Abstract

DC-DC converters are now widely used in low- to medium-power ranges. Since the isolated converters offer input and output isolation as well as protection from input side errors, they are used in medium power applications. In this study, an isolated DC-DC converter is used to power up a digital unit subsystem for a space mission. By operating at a switching frequency of 140 kHz, the suggested converter can use smaller magnetic components. The suggested topology modifies the duty cycle for an input variation using voltage feed forward control. It contains integrated EMI filters to reduce noise coming from adjacent components and vice versa. Cross regulation is a difficult challenge to meet, and this is accomplished by keeping the secondary feedback circuit in a stable zone. Hybrid Micro Circuits (HMC), which decrease the size of the converter, are used in the development of a prototype model. More than 65% converter efficiency is the target.

Keywords: DC-DC Converter; Forward converter; Feed forward, Mag-amp, UC2825 PWM controller.

1. Introduction

Nowadays, DC-DC converters are used widely in a variety of applications, including consumer electronics, telecommunications, industrial, medical, and space. The most important requirements for space mission applications are high reliability and light weight design, not conversion efficiency. Despite the fact that many topologies, including full bridge, half bridge, and push pull DC-DC converters, are capable of high efficiency, their dependability is constrained by the high side switch design. The converter performs well in situations demanding high output currents and moderate to medium power levels. In applications requiring large output currents and moderate to medium power levels, the converter performs admirably. To improve performance, voltage mode with feed forward control has been used. Operating Switching Frequency is 140kHz, Feed forward control mechanism to improve the performance Mag Amp based Post Linear regulator to provide output specifications, Built in EMI/EMC filter, Under I/P Voltage and Short circuit protection, Output Over Voltage Protection, Output TM Status Monitoring, Relay status Monitoring there are some salient features.

1.1. Problem definition

Cross regulation has an impact on the output of a forward DC/DC converter, which not only reduces the efficiency but also impacts the converter's performance. Along with cross regulation, load regulation and line

regulation also impair the performance of the converter. The duty cycle control method using voltage feedback is dynamically slow, which creates line transients that have an impact on the converter's switching performance.

1.2. Objectives

To get over the drawbacks of the dual output forward converter It uses a voltage feed-forward control approach to enhance line transients. On the secondary side, mag-amp is also employed to meet load regulation and line regulation requirements. Energy regenerating snubber improves efficiency and lessens stress on the switch.

1.3. Block diagram

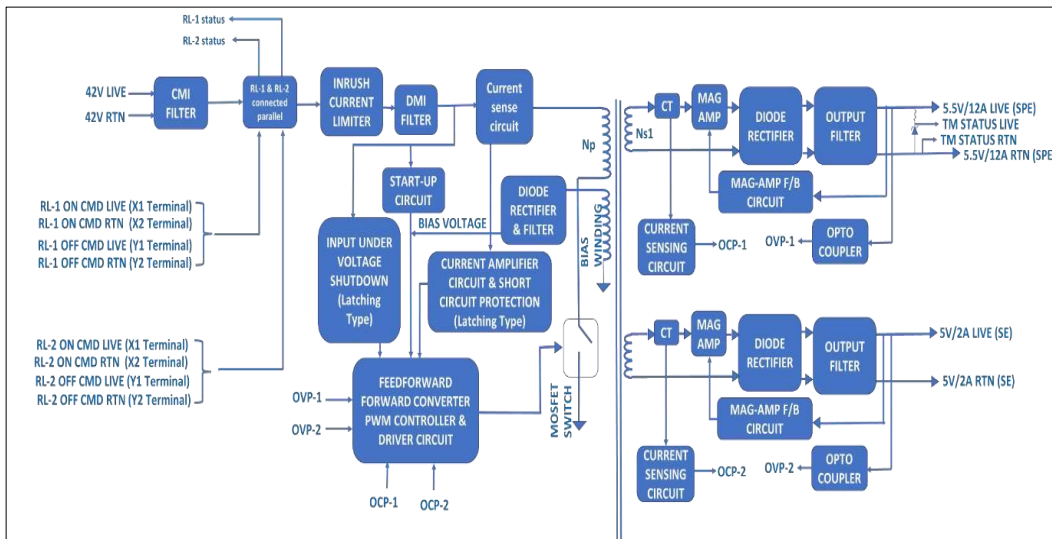


Fig 1. Block Diagram of the proposed converter

1.4. Working

The converter's input card has a voltage feed-forward-controlled MOSFET switch, an EMI filter, an inrush current limiter, a current sense circuit, a start-up circuit, and an under-voltage protection circuit. The system's noise level is decreased by the EMI filter. With a 100% load applied, an inrush current limiter circuit restricts the input current to less than twice the input current. The converter is shielded from excessive or short circuit current by a current sense circuit. The startup circuit powers on-chip components (ICs) while the bias charges. When the input voltage is less than 24V, the converter is shut off by an under voltage protection circuit. Using a voltage feed forward control approach, the duty of a MOSFET switch is controlled. The ICs were previously supplied on a steadybasis by bias winding. Current transformers, mag-amp circuits, filters, opto-couplers, and excess voltage protection circuits are included on the converter's output card. The converter is turned down when the current transformer detects too much current. As post regulators, mag-amps are used. Smooth output voltage is provided by filters. An opto-coupler is used to isolate the input from the output. When the output voltage exceeds 6.6V, an over voltage protection circuit shuts down the converter.

1.5. Specification of the Converter

The Forward Converter specifications are shown in

Table 1 Table I. Forward Converter Specification

Parameters	Specification
Input voltage	24-42.5 V(36V Nominal)
Ripple	<30mVp-p
Output-1	5.5V/12A
Output-2	5V/2A
Output Power	76W
Efficiency	>65%
Switching Frequency	140±5 KHz
Ripple	<30mVp-p
Line Regulations	<±1%
Load Regulations	<±2%

1.6. Design Procedure

In this section design of a) transformer b) criteria for selecting MOSFET switch c) snubber circuit selection d) output filter design e) mag-amp design have been explained. The best component choices are needed to make converters efficient.

a) Transformer Design

The transformer core is chosen using the area product computation. Finally, the smaller size and lower power dissipation of the transformer determine the best design.

Area product calculation (1);

Selected POT Core: OR43019UG, AL: 6682nH/1000 Turns Kw=0.4, J=4Amp/m², Bm=0.08Telsa, Pout=41.2Watts

$$A_p = \frac{\sqrt{D_{max}} \cdot P_{out} \cdot \left(1 + \frac{1}{\eta}\right)}{K_w \cdot J \cdot 10^{-6} \cdot F_{sw} \cdot B_m} \quad (1)$$

Where, i) Kw : Window factor. ii) J: Current density A/mm². iii) Fsw : Switching frequency Hz. iv) Dmax :Maximum duty cycle. v) Efficiency. vi) Bm: Maximum flux density T

The best transformer design uses Kw, Bm, and J. In the end, the transformer's compact size and low power dissipation determine the best design. Kw, Bm, and J are optimized by the designer for these purposes.

Primary turns are calculated from equation (2)

$$N_p = \frac{V_{in} \cdot D_{max}}{B_m \cdot A_c \cdot 10^{-6} \cdot F_{sw}} \quad (2)$$

To know secondary turns, turns ratio to be calculated using formula (3)

$$T_{ratio} = \frac{N_p}{N_s} = \frac{V_{out} + V_d * D_{max}}{D_{max} * V_{in}(\min)} \quad (4)$$

Where, i) V_d : Diode drop. ii) $V_{in}(\min)$: Minimum input voltage

Hence, $N_s = T_{ratio} * N_p$

b) MOSFT selection

As the switch for SMPS applications, the MOSFET is frequently chosen. Power Mosfets are primarily carrier devices that switch at higher frequencies and are faster than bipolar transistors. A voltage-controlled device known as a metal oxide semiconducting field effect transistor is typically employed as an amplifier or switch. It is regarded as one of the most important electronic gadgets for bringing about the modern electronics revolution. This Semiconducting switch is used in many different processes, notably those that involve power conversion. The most frequent reason for failure of high-power circuits like converters and inverters, though, is a power MOSFET. A power MOSFET might fail for a number of reasons, but the most common is choosing the incorrect power MOSFET for the job. Source, drain, and gate are the three terminals on a MOSFET, which is a voltage-controlled 3-terminal device. The three terminal device's fundamental principle is to precisely regulate the voltage between the other two terminals while simultaneously managing the current flow through one of its terminals.

Mosfet selection parameters, Select MOSFET with lowest $R_{ds(on)}$ to reduce the conduction losses, The maximum drain source voltage (V_{ds}), Maximum drain current, Gate source voltage (V_{gs}), Gate source Threshold (V_{th}), Gate charge (Q_g), Low output capacitance (C_{oss}), Maximum allowable power dissipation for the package, Operating temperature .

IRHM57260 is selected which has $V_{DS} = 200V$, $R_{DS(on)} = 49m\Omega$, $I_{Dmax} = 35A$ and $V_{GS(th)max} = 4V$.

c) Diode selection

To reduce conduction and switching losses, use Schottky diodes in low voltage applications up to 100V. For applications requiring higher voltage, use ultra-fast diodes. For high voltage applications, silicon carbide rectifier is another option. Selection of the output diode is influenced by secondary voltage and current. Due to their high current capacity and extremely low forward voltage drop, Schottky diodes are typically ideal.

d) Snubber design

The leakage power loss from the MOSFET is recovered via a lossless snubber (LCD snubber). It lessens the mosfet's switching off loss. Two diodes, an inductor, a capacitor, and a lossless snubber are all included in a liquid crystal display (LCD). By calculating the area product as given in equation, the appropriate core for the inductor is chosen. The selected core is **C055291A2 with $AL = 32nH/T^2$** .

e) Feed forward Voltage mode control

Voltage feedback technique is one of the frequently used methods for regulating the duty cycle of the switch. However, this method is discovered to be dynamically sluggish and also produces poor line regulation. The input voltage feed-forward approach reacts to the signal control and is independent of load change. If there is an abrupt change in output voltage, this method offers superior line transient protection.

By having the slope of the ramp waveform proportional to input voltage, voltage feed forward is achieved. As a result, the duty cycle modulation is matching and correcting without the feedback loop having to take any action. As a result, the duty cycle modulation is matching and correcting itself without the need for any intervention from the feedback loop.

f) Mag –Amp design

A magnetic amplifier is actually a saturable inductor. The mag-amp concept can be explained using a simple LR circuit like the one in Fig.2

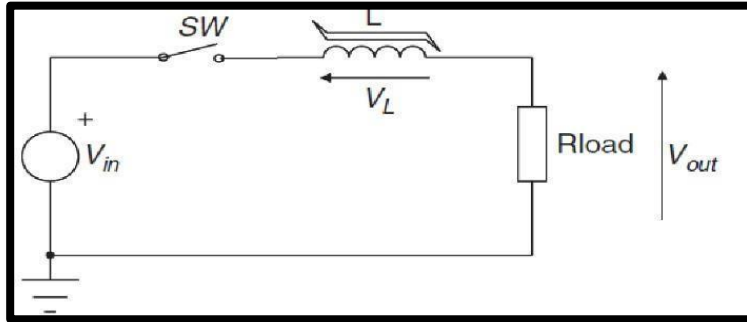


Fig 2: Circuit for Mag-Amp design

The voltage across the load resistor is delayed when a saturable core connected in series with the input source eventually reaches saturation.

An inductor offers a high permeability (μ) and consequently a high inductance when a series switch closes because of its innate ability to resist a rapid shift in current. Across the coil terminals, the entire applied input voltage is visible. Due to the saturable core, the current builds up quickly and saturates it. The inductor appears to be short circuited due to the increase in permeability from μ to 1. After the time delay required to saturate the core, the entire input voltage appears across the resistor R. How long it takes to saturate the core depends on how long it takes for the flux density B to rise from a starting stored value (B_0) to the saturation level, where the inductance collapses. If the development of the flux density is assumed to be linear and the voltage across the saturable inductor is constant at the time of turn-on, the saturation flux density may be represented as follows:

$$B_0 + \frac{V_L \times t}{N_L \times A_e} = B_{sat} \quad (1)$$

$$\Delta t = \frac{(B_{sat} - B_0) N_L \times A_e}{V_L} \quad (2)$$

where A_e is the cross sectional area of the core, B_{sat} is the saturation flux density, B_0 is the starting flux density, N_L is the number of turns on the saturable inductor core, and V_L is the inductor voltage. Equation (2) reveals the Mag-amp's basic functioning principle. All the variables in equation (2) are constants with the exception of B_0 . By altering the point B_0 from which the magnetizing process commences, it is possible to change the amount of time needed to saturate the core. This strategy for regulating the output voltage was carefully considered.

Selected core is 6-L2016-W763, Nanocrystalline Vitroperm 500Z, Square Loop Core

g) Output filter design

For the output voltage waveform to have the necessary quality, the secondary voltage of the transformer is rectified and filtered appropriately. The diode chosen for rectification ought to have a quick switching action and a quick time recovering from reverse. Consequently, an appropriate Schottky diode is chosen. To create a cost-effective, less-bulky power supply, the values of the filter inductor and capacitor must be selected appropriately. The filter capacitor only provides the switching frequency's ripple (ac) current. The output voltage and switch duty ratio have a linear relationship, and constant inductor current is preferred.

The L and C values are designed using the following equations.

$$L = \frac{V_o*(1-D_{min})*T_s}{\Delta iL} H$$

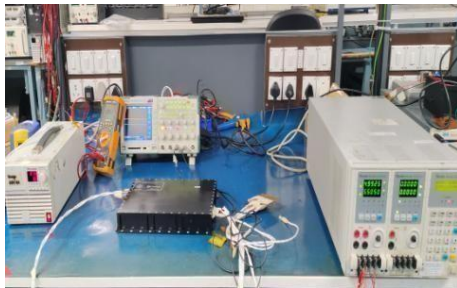
From above equation L1 = 12.1µH and L2 = 18µH are calculated values for master and slave outputs respectively.

$$C = \frac{1-D_{min}}{8*L*F_{sw}^2*\delta V_o}$$

Similarly, C1 = 940µF and C2 = 470µF are the filter capacitances.

2. Experimental results

The below figures demonstrate the experimental setup and the forward converter's top view. An electronic load that measures the output voltage and load current is connected to the converter's output and is used to power it up. A digital storage oscilloscope (DSO) is connected to detect output ripple.



a) Experimental Setup



b) Top view of the forward converter when the load is at 100%

The measured outputs at full load are quite close to the specified values, and an efficiency of more than 65% is attained.

Table II. Output at 100% load

Vin (V)	Iin (A)	V01 (V)	Io2 (A)	V02 (V)	Io2 (A)
24	4.341	5.447	12	4.979	2
36	2.911	5.451	12	4.979	2
42.5	2.485	5.451	12	4.978	2

Outputs at a 10% minimum load condition

When outputs are tested under minimum load conditions, the numbers are almost identical to those that were prescribed since the drop is lower.

Table III. Output at 10% load

Vin (V)	Iin (A)	V01 (V)	Io2 (A)	V02 (V)	Io2 (A)
24	0.604	5.509	1.2	5.001	0.2
36	0.435	5.508	1.2	5.001	0.2
42.5	0.383	5.508	1.2	5.000	0.2

Efficiency with full load condition

Table IV. Efficiency with full load condition

Input Voltage(V)	Input Power(W)	Output Power(W)	Efficiency(%)
36	104.80	75.37	71.96

Line Regulation

A line regulation of 1% is accomplished on both outputs by using the feed-forward control approach.

Table V. Line regulation at different loads

Load	Line Regulation(±1%)	
	+5.5V/12A	+5V/2A
100%	-0.073	0.02
50%	-0.036	0
10%	0.018	0.02

Load Regulation

With the aid of post regulators mag-amps, the output voltage fluctuations caused by changes in load current are kept to a minimum (2%).

Table VI. Load regulation at different loads

Load	Load Regulation(±2%)	
	+5.5V/12A	+5V/2A
100%	0.656	0.220
50%	0.601	0.224
10%	0.619	0.240

Ripple Waveforms

For both outputs, the ripple is measured under full load conditions, and the measured value is less than the target value of 30 mVp-p.

Ripple at 100% Load and 42.5V input O/P-1

5.5V = 20mV

O/P-2 5V = 14mV

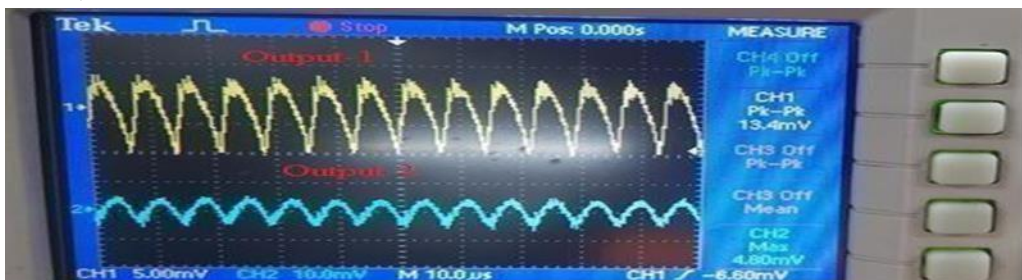


Fig3; Ripple at 100% load

Ripple at 10% Load and 42.5V input

O/P-1 5.5V = 13.4mV

O/P-2

5V

=4.80mV

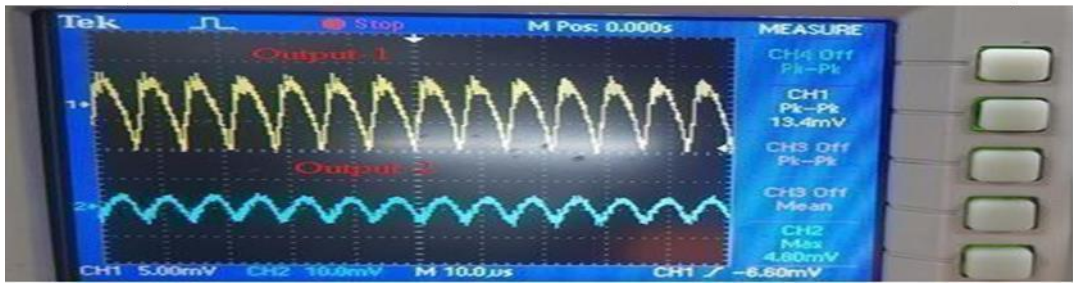


Fig 4; Ripple at 100% load

Fig. illustrates the gate to source voltage (VGS) and drain to voltage source (VDS) under full load and a 42.5V input voltage. The converter is working at the appropriate frequency (140 kHz), and the usage of the snubber circuit limits the stress on the MOSFET to less than twice Vpeak.

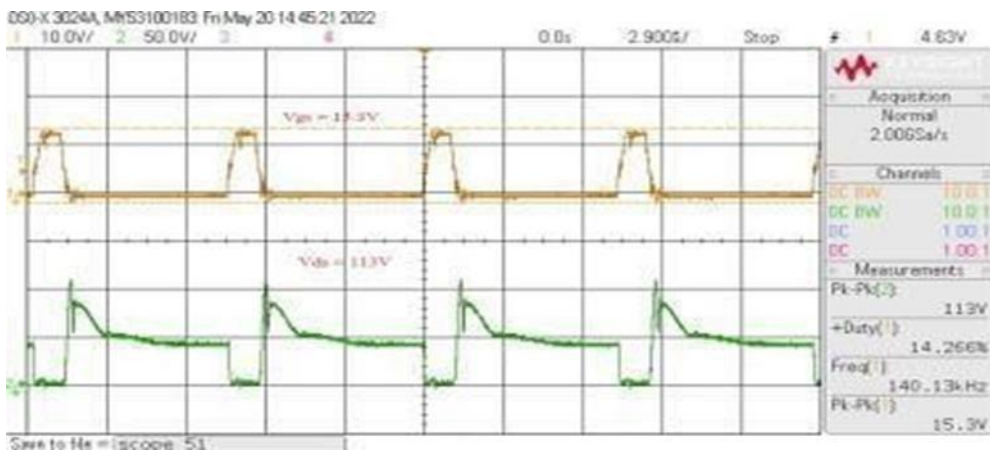


Fig5; Vgs and Vds Waveforms at 42.5V Input Voltage

Transients in the voltage and currents may be briefly visible when the converter is hooked in. At 42.5V input voltage, inrush current is shown in Fig. The current is restricted to less than twice the input current with the aid of an inrush current limiter circuit, and it reaches steady state within the allotted period of 6 msec.



Fig 6; Inrush Current at Maximum Voltage (42.5V)

The voltage briefly overshoots or undershoots when the load changes dramatically or abruptly. The load transient response is seen in Fig at 36V input. It overshoots by 32mV and 30.4mV, both of which are below the desired value.(5% of the output voltage or 250mV-P).

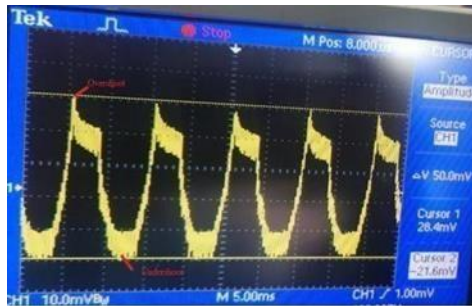


Fig 7; Load Transient of O/P-1(5.5V/12A) at 36V Input



Fig 8; Load Transient of O/P-2(5V/2A) at 36V Input

3. Conclusion

The converter prototype model is created and put through rigorous testing to meet all the chosen parameters. Better load regulation for controlling individual outputs is provided by the mag-amp regulation method. Using the voltage feed forward control approach line 1% control because it provides quick dynamic reaction.

Acknowledgment

Authors are thankful to the Management, B.M.S Educational Trust, Principal and Vice Principal, BMS College of Engineering and Centum electronics Ltd. for their continuous support.

References

- [1] N. Lee, J. -Y. Lee, Y. -J. Cheon, S. -K. Han and G. -W. Moon, "A High-Power-Density Converter with a Continuous Input Current Waveform for Satellite Power Applications," in IEEE Transactions on Industrial Electronics, vol. 67, no. 2, pp. 1024-1035, Feb. 2020, doi: 10.1109/TIE.2019.2898584.
- [2] Youhao Xi and P. K. Jain, "A forward converter topology with independently and precisely regulated multiple outputs," in IEEE Transactions on Power Electronics, vol. 18, no. 2, pp. 648-658, March 2003, doi: 10.1109/TPEL.2003.809348.
- [3] C. Xu, Q. Ma, P. Xu and N. Wang, "Closed-Loop Gate Drive for Single-Ended Forward Converter to Reduce Conducted EMI," in IEEE Access, vol. 8, pp. 123746-123755, 2020, doi: 10.1109/ACCESS.2020.3005239.
- [4] N. Lee, T. -Y. Kim, J. -Y. Lee, S. -K. Han, T. -J. Chung and J. -D. Choi, "Improved EMI noise performance by the reduced input ripple of the Satellite converter," 2019 European Space Power Conference (ESPC), 2019, pp. 1-5, doi:

10.1109/ESPC.2019.8932057.

- [5] J. -Y. Lin, S. -Y. Lee, C. -Y. Ting and F. -C. Syu, "Active-Clamp Forward Converter with Lossless- Snubber on Secondary-Side," in IEEE Transactions on Power Electronics, vol. 34, no. 8, pp. 7650-7661, Aug. 2019, doi: 10.1109/TPEL.2018.2879721.
- [6] A. Bhat, K. U. Rao, Praveen P K, B. K. Singh and V. Chippalkatti, "Multiple output forward DC-DC converter with regenerative snubber for space application," 2016 Biennial International Conference on Power and Energy Systems: Towards Sustainable Energy (PESTSE), 2016, pp. 1-5, doi: 10.1109/PESTSE.2016.7516487
- [7] A. Bhat, K. U. Rao, Praveen P K, B. K. Singh and V. Chippalkatti, "Multiple output forward DC-DC converter with Mag-amp post regulators and voltage feedforward control for space application," 2016 Biennial International Conference on Power and Energy Systems: Towards Sustainable Energy (PESTSE), 2016, pp. 1- 6, doi: 10.1109/PESTSE.2016.7516488.
- [8] Nagaraju T K, Aneesh and Bharath T K "Design and performances challenges of power supplies for space " 2011 IEEE International Vacuum Electronics Conference (IVEC), 2011, pp. 431-432, doi: 10.1109/IVEC.2011.5747060.
- [9] Y. Lu, T. Liang, C. Lin and K. Chen, "Design and implementation of a bidirectional dc-dc forward/flyback converter with leakage energy recycled," 2017 Asian Conference on Energy, Power and Transportation Electrification (ACEPT), 2017, pp. 1-6, doi: 10.1109/ACEPT.2017.8168572.
- [10] B. Singh and G. D. Chaturvedi, "Comparative Performance of Isolated Forward and Flyback AC-DC Converters for Low Power Applications," 2008 Joint International Conference on Power System Technology and IEEE Power India Conference, 2008, pp. 1-6, doi: 10.1109/ICPST.2008.4745255
- [11] Huang, M., Wang, C., Liu, B., Wang, F. and Wang, J., 2020. Quadrature Kalman filter-based state of charge estimation for lithium-ion battery. *Advances in Mechanical Engineering*, 12(7), p.1687814020942696.
- [12] KM Naresh, M Umavathi, HR Mohan, Multi output Fly back Converter with Switching/Linear Post Regulators, International Journal of Recent Development in Engineering and Technology, pp 21 26 ISSN 2347 -6435, Vol. 6, Issue 6, 2014.
- [13] Umavathi M & Suresh S, Ekambe PLECS Software for UPS Application Using Isolated Bidirectional DC-DC Converter,Lino,2020.